Electronic Supplementary Material (ESI) for Journal of Materials Chemistry A.

Supplementary information

Determination of the ion-conduction properties of Na_3OBr and its dominant defect species

Reona Miyazaki[1*], Shiori Ito[1], Kana Ishigami[2], Hidetoshi Miyazaki[1], and Takehiko Hihara[1]

1 Department of Physical Science and Engineering, Graduate School of Engineering,

Nagoya Institute of Technology, Gokiso-cho, Showa, Nagoya 466-8555, Japan

2 Creative Engineering Program, Graduate School of Engineering,

Nagoya Institute of Technology, Gokiso-cho, Showa, Nagoya 466-8555, Japan

1. Particle morphology of the Na_2O/Na mixed powder

Na_2O (purity 80 %, Aldrich) and pieces of Na metal were mixed by S. S. mortar, resulting in a fine mixed powder. Fine powders with several micro meters were aggregated and coalesced.

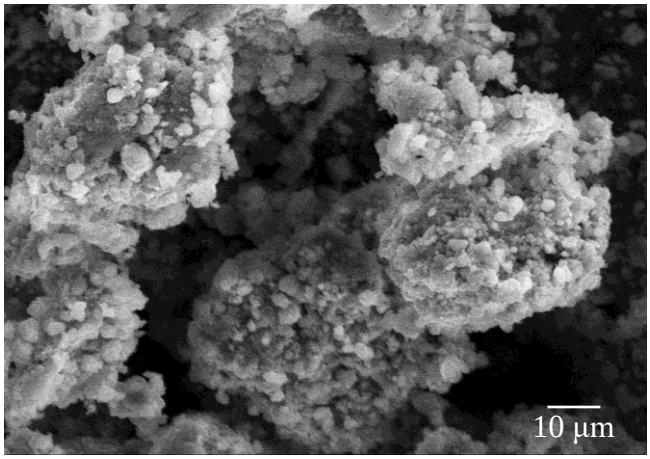

Figure S1: SEM image of Na_2O/Na mixed powder before the purification

2. XRD patterns of Ca^{2+}-doped Na_3OBr

Fig. S2(a) shows XRD patterns of Ca^{2+}-doped Na_3OBr. Compositional dependence of lattice parameters and 110 peak widths are presented in Fig. S2(b). Lattice parameter of Na_3OBr was decreased for lower Ca^{2+} concentration, which is explained by the substitution of Na^+ (1.02 Å) by smaller Ca^{2+} (1.00 Å). On the other hands, further increase of Ca^{2+} concentration resulted in the lattice expansion. By increasing Ca^{2+} concentration, the peak widths were broadened although the samples were post-annealed under the same conditions (350 °C for 2 hours). The lattice disordering by vacancies has been reported for *e.g.*, ion-irradiated CeO_2 [*Quantum Beam Sci*. 2020, **4**, 26]. Although the relation between the lattice disordering and the cation vacancies in Na_3OBr has not been specifically investigated, at present, we believe that the peak broadening for higher Ca^{2+} concentration is owing to the increase of Na^+ vacancies. The results in Fig. S2 indicate the positive correlation between the peak broadening and the lattice expansion by Ca^{2+} doping. The increase of lattice parameters by vacancies has been reported for some ceramics (*e.g.*, CeO_2 and KCl) [*Thin Solid Films*, 207 (1992) 288, C. Kittel, *Introduction to Solid State Physics 7th edition*, *Chap*. 18, 542-543]. Hence, it is predicted that cation vacancies contribute for the expansion of Na_3OBr lattice. The non-linear variation of the lattice parameters in Fig. S2 can be explained by the competing effects of the substitution of Ca^{2+} ions (lattice shrinkage) and the introduction of cation vacancies (lattice expansion).

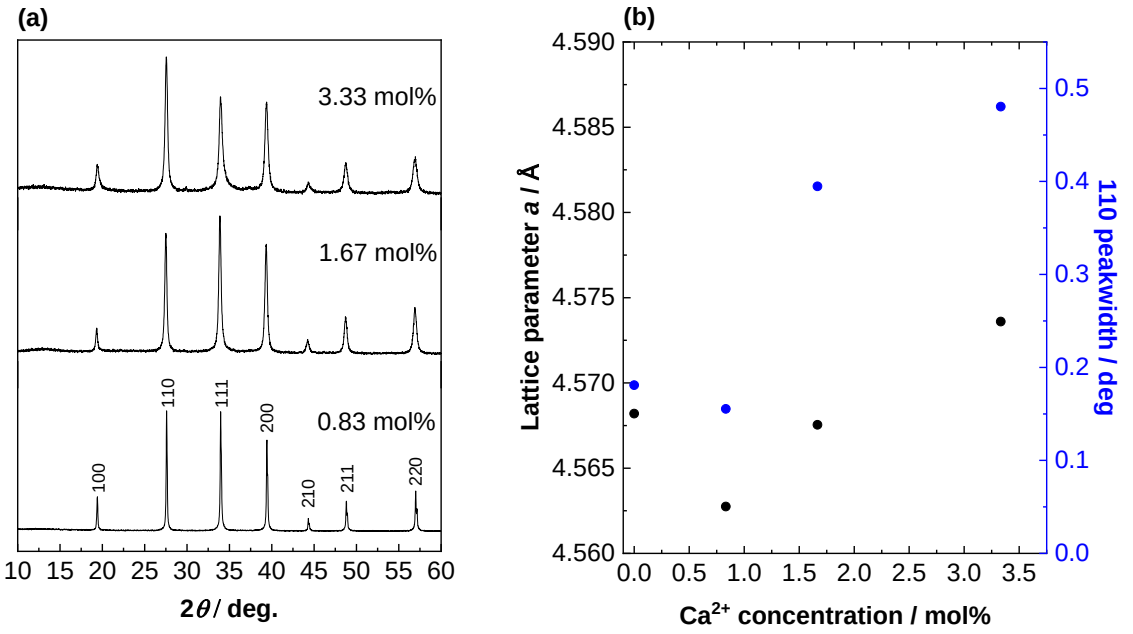

Figure S2: XRD patterns of Ca^{2+}-doped Na_3OBr. Bottom, middle and top data represent the Ca concentration of 0.83, 1.67 and 3.33 mol%, respectively. (b): Compositional dependence of lattice parameters (black) and 110 peak widths (blue).

3. Variations of the relative peak intensity ratio of Na_3OBr with/without excess Br^- on O^{2-} sites

The relative intensities of the diffraction peaks of Na_3OBr were clearly changed by introducing the excess Br^- on O^{2-} sites with Na vacancies. The most significant variation is the intensity ratio of 110/111 peaks. Relative intensity of 110 was increased for Na_3OBr with the excess Br^- (5 mol%) on O^{2-} sites and Na vacancies (5 mol%) compared to the perfect crystal.

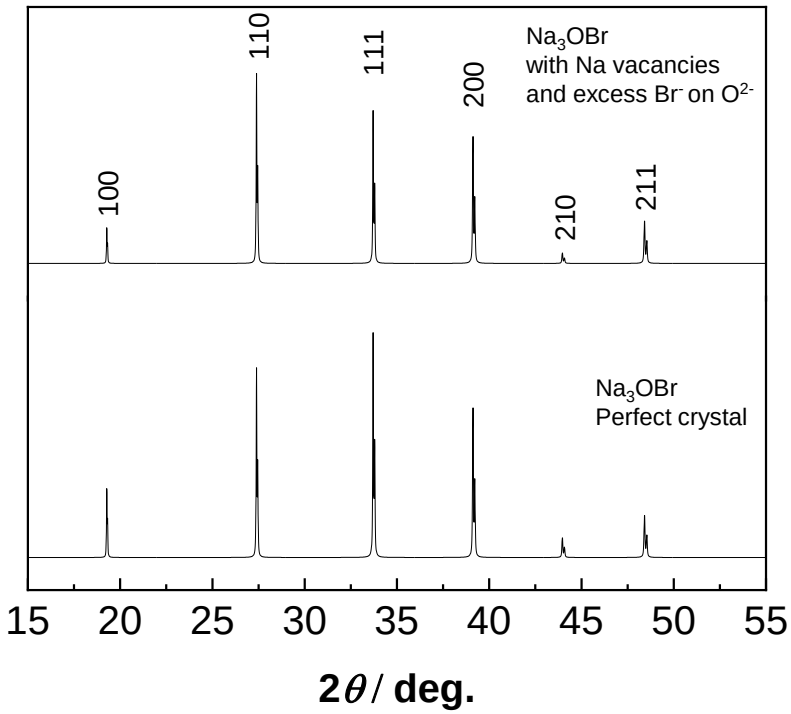

Figure S3: Simulated XRD pattens of Br^--rich and perfect Na_3OBr

4. Compositional dependence of the lattice parameters for Br^--rich Na_3OBr

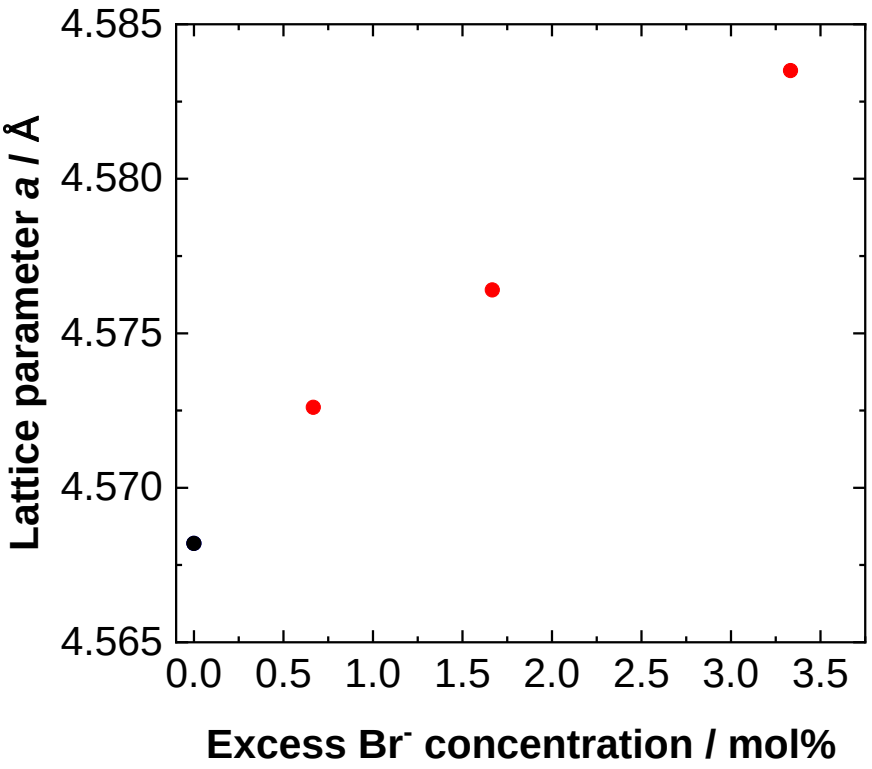

Figure S4: The lattice parameters of Na_3OBr with excess Br^- concentration. The data for non-doped Na_3OBr is plotted by black circle.

5. XRD pattern of Ca^{2+}-doped Na_3OBr after sintering above 400 °C

To densify the pellet, Ca^{2+}-doped Na_3OBr was sintered at 600 °C for 1 h in a glove box. After sintering, *RP* phase (Na_4OBr_2) was observed, indicating the decomposition of *AP* phase. The segregation of the *RP* phase (Br-rich phase) indicates the presence of residual Na_2O followed by the decomposition reaction ($2Na_3OBr \rightarrow Na_4OBr_2 + Na_2O$). However, diffraction peaks of Na_2O were not confirmed in this study. The detailed mechanism of the phase separation into *RP* and *AP* phases has not been understood.

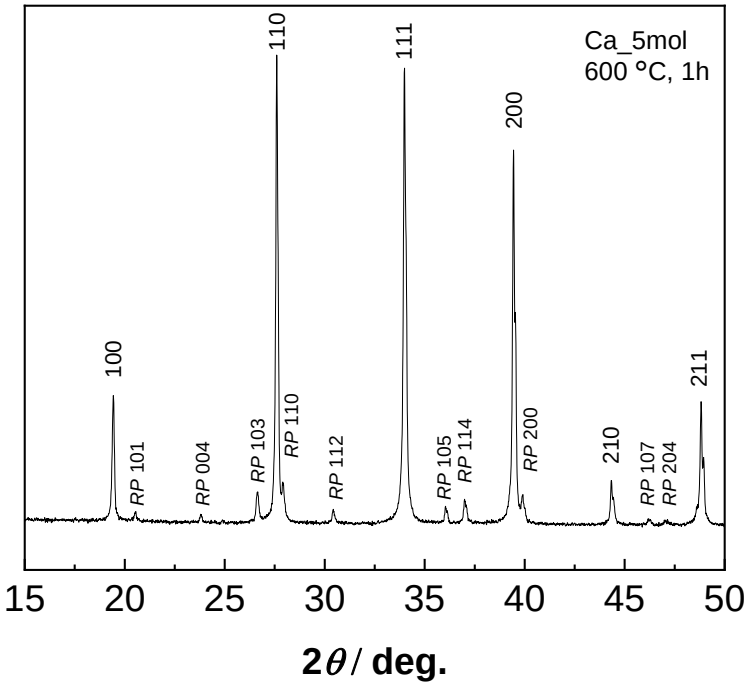

Figure S5: XRD pattern of Ca^{2+}-doped Na_3OBr after sintering at 600 °C in a glove box

6. Crystallite size and lattice strain of Na_3OBr

Crystallite size and lattice strain of as-milled, sintered at 400 °C and hot-pressed Na_3OBr were estimated from the peak width of XRD patterns. The calculations were based on the data obtained by MiniFlex (λ = 1.54 Å).

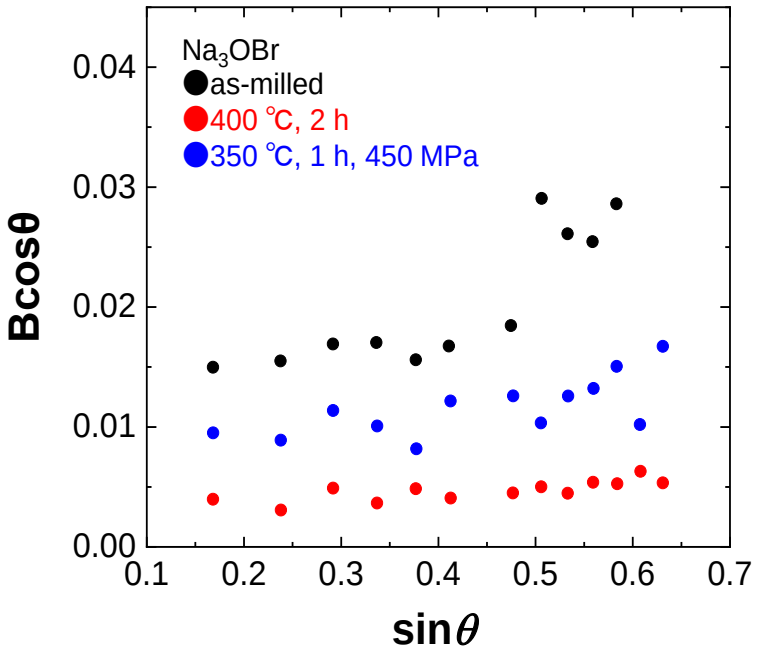

Figure S6: Williamson-Hall plots of Na_3OBr prepared under three conditions

Table S1: Crystallite size and lattice strain of Na_3OBr estimated from Williamson-Hall plots

Na_3OBr	**Crystallite size / nm**	**Lattice strain**
As-milled	22	0.032
400 °C, 2h	55	0.0044
350 °C, 1h, 450 MPa	23	0.0112

7. Variation of the crystalline phase after conductivity measurement

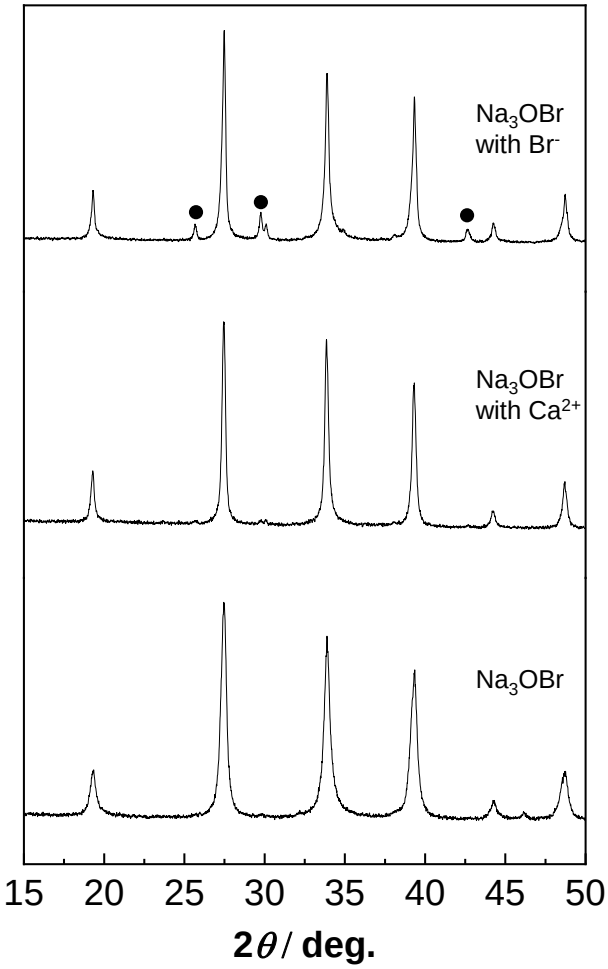

Figure S7: XRD patterns of Na_3OBr-based materials after conductivity measurement. Diffraction peaks of NaBr are presented by black circles.